Neurotherapeutics 21 (2024) e00429

Contents lists available at ScienceDirect

Neurotherapeutics

journal homepage: www.sciencedirect.com/journal/neurotherapeutics

Original Article

Long non-coding RNA SNHG12 regulates leptomeningeal collateral remodeling via RGMa after ischemic stroke

Anan Jiang [1], Zijie Wang [1], Ruiqi Cheng [1], Shaoru Zhang [1], Qisi Wu [*], Xinyue Qin [*]

Department of Neurology, The First Affiliated Hospital of Chongqing Medical University, Chongqing 400016, China

ARTICLE INFO

Keywords:
Ischemic stroke
SNHG12
Leptomeningeal collateral remodeling

ABSTRACT

Leptomeningeal anastomoses or pial collateral arteries are crucial for restoring cerebral blood flow (CBF) after an ischemic stroke. Vascular smooth muscle cells (VSMCs) are hypothesized to regulate the extent of this adaptive response, while the specific molecular mechanisms underlying this process are still being investigated. SNHG12, a long non-coding RNA, has been shown to influence several diseases related angiogenesis, including osteosarcoma and gastric cancer. However, the role of SNHG12 in contractile VSMC dedifferentiation during collateral arteriogenesis-related strokes remains unclear. Here we demonstrated that SNHG12 is a positive regulator of MMP9 and VSMC dedifferentiation, which enhances pial collateral arteriogenesis following cerebrovascular occlusion. Pial collateral remodeling is limited by the crosstalk between SNHG12-MMP9 signaling in VSMCs, which is mediated through repulsive guidance molecule a (RGMa) regulation. Thus, targeting SNHG12 may represent a therapeutic strategy for improving collateral function, neural tissue health, and functional recovery following ischemic stroke.

Introduction

Ischemic stroke is defined as a decrease in cerebral blood flow (CBF) in the brain due to the blockage of the middle cerebral artery (MCA), resulting in neurological deficits. However, the reduction in CBF can be restored by rapid retrograde perfusion of blood flow through the collateral circulation, which connects the vascular network of blood vessels in two different blood-supplying regions. An abundant collateral circulation can protect the ischemic brain tissue, which is strongly linked to patient clinical prognosis. However, the molecular mechanisms underlying the regulation of this collateral circulation have not yet been fully investigated. Revascularization therapies for acute ischemic stroke, such as intravenous thrombolysis (IVT) and endovascular therapy (EVT), are time-dependent, with efficacy decreasing significantly as the appropriate time window passes. However, patients with a stronger cerebral collateral circulation, may have a longer time frame to reap the benefits of reperfusion therapy. Several studies have found that excellent collateral circulation can enhance functional results at 3–6 months, increase reperfusion rates, and lower core infarct volume in patients receiving thrombolytic therapy [1–3]. Therefore, understanding the mechanism underlying vascular collateral remodeling could enhance the efficacy of treatment and prognosis in patients with acute ischemic stroke.

The focus of revascularization is to salvage the ischemic penumbra, the progress of which is regulated by the collateral circulation. Good collaterals enhance brain tissue tolerance to ischemia and hypoxia, while minimizing the ischemic penumbra and infarct size. Thus, treatments that target collateral circulation, particularly molecular pathways, represent a feasible therapeutic option for improving the prognosis after stroke by sustaining penumbral blood flow and neural tissue function. Leptomeningeal anastomoses (LMA) connect the MCA region to the anterior cerebral artery (ACA) and posterior cerebral artery (PCA) to ensure blood supply. Certain branches of the network can further connected to arteries near the ischemic tissue, thereby enabling reverse perfusion of blood flow to supply the ischemic area. Follwing stroke, the collateral arteries undergo vascular remodeling (enlargement), also known as arteriogenesis, which allows unidirectional retrograde blood reperfusion to the obstructed arterial branch.

In recent years, several breakthroughs in our understanding of arteriogenesis have been achieved, while a better understanding of the interactions between physical forces and cellular and molecular pathways has been attained [4]. However, further knowledge of a potential molecular treatment paradigm superior to surgery and angioplasty is still required. The growth process of differentiated collateral arteries is known to dominated by the proliferation of smooth muscle cells,

* Corresponding authors.
E-mail addresses: wuqisi@hospital.cqmu.edu.cn (Q. Wu), QXYqinxinyue@163.com (X. Qin).
[1] Co-authors: Anan, Jiang, Zijie, Wang, Ruiqi, Cheng, Shaoru, Zhang these authors contributed equally to this article.

https://doi.org/10.1016/j.neurot.2024.e00429
Received 31 March 2024; Received in revised form 26 July 2024; Accepted 26 July 2024

adventitial fibroblasts, and endothelial cells. Thus, smooth muscle cells in collateral ecotopes can play a critical role in active remodeling. Recently, reserach in our team showed that the long noncoding (lnc) RNA SNHG12 is associated with collateral arteriogenesis following cerebral ischemia-reperfusion in mice. MMP9, a zinc-dependent metalloproteinase, is generally expressed at low levels in normal adult tissues, but is significantly upregulated during vascular remodeling. In the persent study, we further show that smooth muscle cells play major roles in the lateral branch remodeling in the leptomeningeal region following ischemic stroke, and that SNHG12 promotes these growth properties via the RGMa/MMP9 signaling pathway both in vitro and in vivo. Overall, these findings greatly improve our understanding of the cellular and molecular mechanisms involved in pial collateral remodeling after vascular obstruction.

Materials and methods

Animals and surgical procedures

The animal experiment was approved by the Institutional Animal Care and Use Committee (IACUC) of the First Affiliated Hospital of Chongqing Medical University. Male C57BL/6J mice (20–22 g) from Chongqing Medical University's Animal Research Center were housed in a pathogen-free environment with 22 ± 2 °C, 50%–70% relative humidity, 12 h light/12 h dark cycle, and free access to food and drink. Experiments were carried out after one week of acclimation feeding. The adenoviral vector (pAdEasy-EF1-MCS-CMV-mCherry) containing the whole RGMa and SNHG12 complementary DNA (cDNA) sequence is designated. 2ul RGMa-specific recombinant adenovirus (Ad-RGMa, 2×10^{10} plaque-forming unit/ml; Genechem Co, Ltd, China), SNHG12-specific recombinant adenovirus (Ad-SNHG12, 2×10^{10} plaque-forming unit/ml; Hanbio Biotechnology Co. Ltd, China) or EGFP carrier recombinant adenovirus (Ad-NC, 2×10^{10} plaque-forming unit/ml) were applied to the Bilateral ventricles.

Ischemic stroke was induced by middle cerebral artery occlusion reperfusion

(MCAO/R) as previously described [5]. Before the operation, the mice were given a 3% pentobarbital solution and allowed to starve for 12 h while still having access to water. Wire embolization established the middle cerebral artery blockage or reperfusion model. Following sterilization, the skin was cut in the middle of the neck to reveal the right common carotid artery (CCA), internal carotid artery (ICA), and external carotid artery (ECA). The proximal end of the CCA and the distal end of the ECA were tied, and a tiny incision emerged in the CCA to insert the monofilaments into the ICA. After a slight resistance, the monofilaments were stopped and tied with a silk knot above the CCA incision. Following an hour of ischemia, the monofilaments were withdrawn, and the live knot on the CCA was tightened for reperfusion.

Vessel painting and collateral quantification

Post-anesthesia with 3% pentobarbital, mice received heparin (2000 units/kg) and sodium nitroprusside (SNP, 0.75 mg/kg) [6]. After stopping breathing, mice were given 10 ml of 1x phosphate-buffered saline (1x PBS) with 20 units/ml heparin to flush blood, followed by 10 ml of DiI (0.01 mg/ml, Invitrogen) diluted in 4% sucrose–PBS-heparin at 2 ml/min to label arteriole vasculature, and finally fixed with cold 4% paraformaldehyde (PFA). Following perfusion, the brains were carefully removed from the skull and stored in PFA overnight. Fixed brains were scanned at 4x magnification using multiple image planes on a Nikon Confocal microscope (BX-51, Olympus America) with mosaic tile imaging from NIS Elements viewer. Images were imported into ImageJ (NIH) to calculate the number and diameter of inter-collaterals, as described [7]. Similarly, the number of $PCNA^{+}/VP^{+}$ cells within the collateral vessel walls was quantified using ImageJ's cell-counting tool from maximal Z-projected images.

Immunohistochemistry of cortical whole mounts

Cortical whole mounts were dissected and stored in 1X PBS overnight, as previously described [7]. Whole mounts were blocked in 5% BSA (catalog no.: ST023; Beyotime) with 0.1% Triton X-100 and treated at 4 °C overnight in mouse anti-smooth muscle actin (SMA) (1:1000; Abcam, ab7817). Whole mounts were washed, incubated with anti-mouse Alexa Fluor 488-conjugated secondary antibody (Thermo Fisher Scientific), and observed with a Carl Zeiss 880 confocal microscope. PCNA staining was performed on whole mounts as previously described.

Behavioral testing

Rotarod. Mice were pretrained for four days prior to MCAO/R or sham injury at 10 rpm and an acceleration of 0.1 rpm per second for 5 min. On the fourth day, a baseline was collected, followed by tests 1, 3, and 7 days after the injury.

The Modified Neurological Severity Scores (mNSS). The mice were graded on the 1, 3, and 7 days after injury to assess the neurological deficits of each group. mNSS is a composite of exercise test, sensory test, balance test, reflex test, and abnormal exercise [8]. There were 18 points in all, and the greater the score, the more severe the neurological deficiency.

2,3,5-triphenyl tetrazolium hydrochloride (TTC) staining

After 3 days of reperfusion, mice were sacrificed by overdose anesthetic, and the cerebral cortex was removed and stored at −20 °C. After 30 min, remove the brain tissue and chop it into six pieces before incubating it in TCC solution for 30 min at 37 °C. Infarct size was determined by ImageJ (1.37C; Bethesda, MD).

Cerebral blood flow (CBF)

CBF was measured as previously described [7]. CBF was measured before, 5 min after, and 1–4 days after injury using the Moor LDI2-HIR Laser Doppler and Moor Software Version 5.3 (Moor Instruments). Mice were anesthetized with 2% isoflurane-30% O2 and CBF was scanned in PFUs using a 2.5 cm × 2.5 cm scanning area.

A ratio of post-PFUs to the pre-injury scan was used to quantify tissue perfusion in mice using the same standardized region of interest (ROI) on the right hemisphere or injury side.

Culture of primary VSMCs and infection

Cell culture

Primary VSMCs were obtained from the leptomeninges of fetal mice at one day postnatally, as described in the literature [9]. Cells were cultured in DMEMF/12 (catalog no.: A4192001; Gibco, MA) with 10% FBS (catalog no.: 164210-600; Pricella, China) and 1% penicillin/streptomycin (catalog no.: C0222; Beyotime, China). Cells were incubated at 37 °C in a humidified environment containing 5% CO2 and used between generation 3 and 5.

Cell infection

VSMCs were infected with recombinant adenoviruses of suitable titers for RNA and protein expression. Cells were infected with the appropriate titer of each adenovirus diluted in 1 ml of DMEMF/12 with 10% FBS for 16 h at 37 °C. The infection medium was replaced the next day with the standard medium and cultured for one additional day before the experiment. The adenoviral vector (pAdEasy-EF1-MCS-CMV-mCherry) containing the whole RGMa and SNHG12

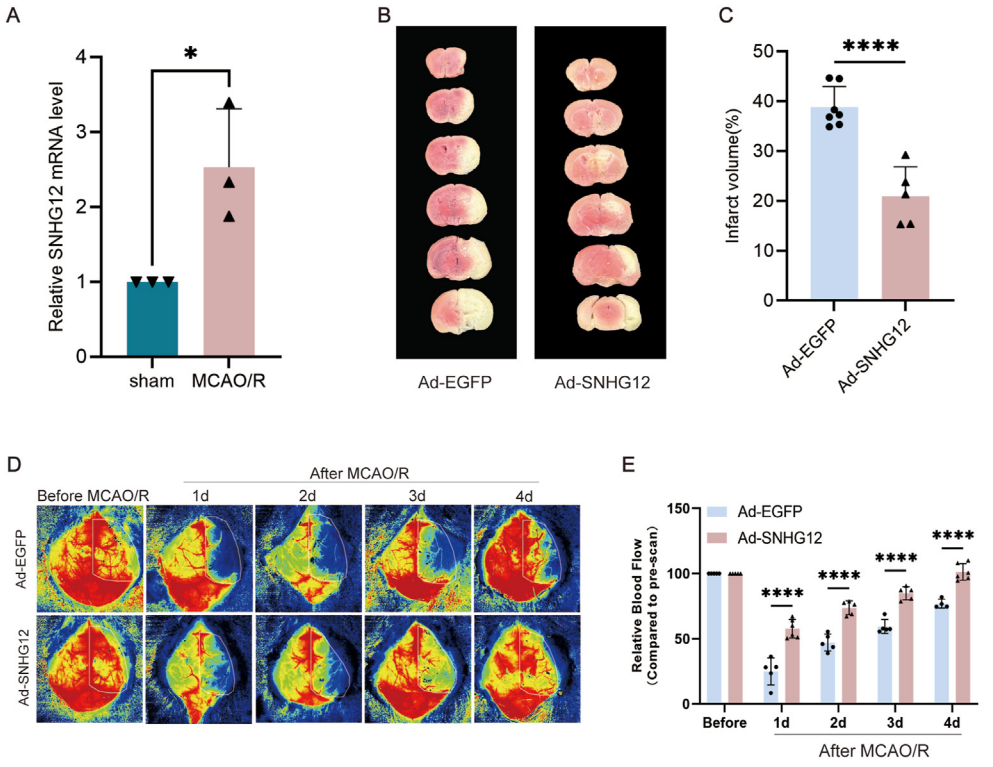

Fig. 1. Increased CBF and decreased infarct volume in Ad-SNHG12 mice after MCAO/R. (A) Following MCAO/R, SNHG12 expression increased; n = 3. (B) TCC staining for determining brain infarct volume. (C) Quantified infarct volume in Ad-SNHG12 mice is significantly lower than in Ad-NC mice; n = 5. (D) Laser Doppler images taken before and after MCAO/R. Panel exhibits Ad-SNHG12 and Ad-NC pictures before and after MCAO/R. (E) Quantified analysis shows Ad-SNHG12 groups have higher CBF than Ad-NC groups; n = 5. (F) Rotarod evaluation of Ad-NC and Ad-SNHG12 groups. Ad-SNHG12 mice outperformed Ad-NC animals at 4 and 7 days post-stroke. G) NSS was assessed 1–7 days after MCAOR. n = 5–6; two-way ANOVA with Bonferroni's post hoc test. $^{*}P < 0.05$, $^{****}P < 0.0001$ compared with matching Ad-NC mice; $^{\#\#\#\#}P < 0.0001$ compared with corresponding sham mice. White dotted lines in D represent the standardized ROI utilized for the CBF quantification of each sample.

complementary DNA (cDNA) sequence is designated. In vitro transfection with siRNAs were performed using Lipofectamine RNAiMax Reagent (catalog no.: 13778030; Invitrogen). Si-RNA against mice RGMa (si-RGMa) and NC (si-NC) were designed and synthesized by GenePharma (Shanghai, China). Si-RNA sequences are as follows: si-RGMa: CGUGCAAGUCACCAAUACA (5′–3′) and UGUAUUGGUGACUUGCACG (3′–5′).

Oxygen-glucose deprivation and reoxygenation (OGD/R)

To imitate the physiological conditions of MCAO/R in vivo, OGD/R was carried out by an established procedure [10]. When primary VSMCs reached 80–90% confluence, the cell culture media was replaced with glucose-free DMEM medium (Gibco, USA), and the cells were placed in a hypoxic incubator with a gas combination of 94% N2, 5% CO2, and 1% O2, which was kept at 37 °C for 6 h. Following that, the cells were returned to the normal growth medium and cultured for 24 h under standard conditions.

Cell migration assay

Wound healing. VSMCs were grown in 6-well plates until 70–80% confluence, then treated with Ad-NC or Ad-SNHG12 for 3 days. Cells were cultured in the presence or absence of OGD/R, and cell migration to the scratched area was determined using a microscope (Leica, Germany) at 0 and 24 h after the test.

Transwell assay. Transwell migration tests were conducted with an 8 μm chamber (catalog no. 3422; Corning). Following Ad-NC or Ad-SNHG12 infection and OGD/R treatment as described above, VSMCs were extracted using 0.25% trypsin (catalog no. C0201; Beyotime) and seeded into the upper chamber. The lower chamber contained 500 μl of media to promote VSMC migration. 12 h later, cells in the top chamber were sterilized with a cotton swab, and migrating cells in the lower chamber were fixed and stained with 0.1% crystal violet (catalog no. C0121; Beyotime). The migrating area was determined using Image-Pro Plus 6.0 (National Institutes of Health) software, and the number of VSMCs in the Transwell chamber was counted.

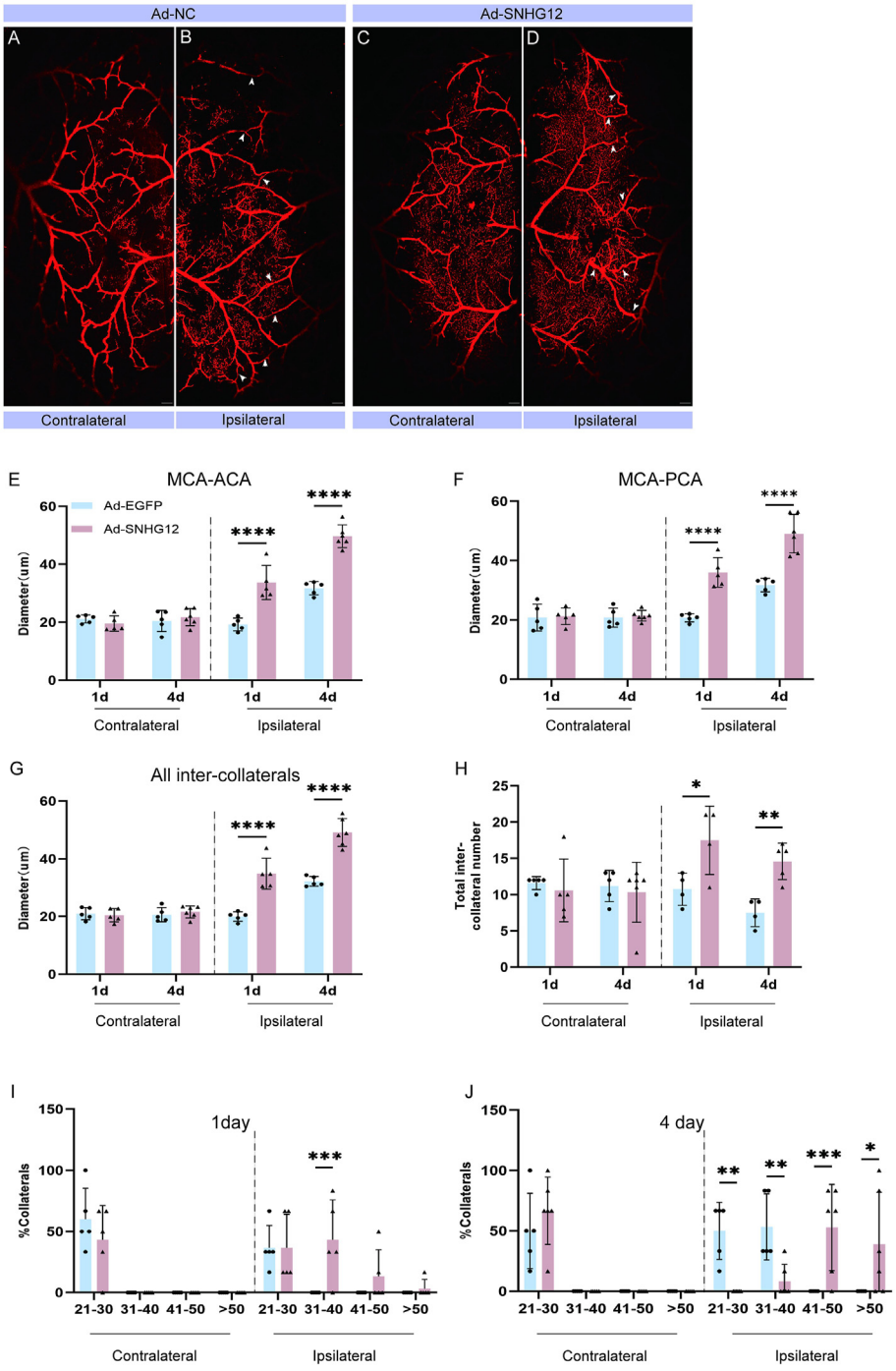

Fig. 2. Increased collateral modification in Ad-SNHG12 mice after MCAO/R. (A and B) Vessel painted Ad-NC brain 1 day after MCAO/R revealing ipsilateral hemisphere pial collateral vessels (arrows). (C and D) Ad-SNHG12 vessel painting was performed 1 day after MCAO/R. (E) Analysis of the collateral diameters of MCA-ACA 1 and 4 days following MCAO/R. The collateral size of Ad-SNHG12 mice is larger than Ad-NC mice (*). (F) MCA-PCA collateral analysis 1 and 4 days following stroke. (G) Significant differences between time points or between the ipsilateral and contralateral hemispheres are revealed by average inter-collateral analyses and (H) inter-collateral counts. The size of the collateral vessel shrank at 1 day (I) and 4 days (J) after MCAO/R. One-way ANOVA with Bonferroni's post hoc test; n = 5 per group. $^{\#, \$}P < 0.05$; $^{**, \#\#, \$\$}P < 0.01$, $^{***, \#\#\#, \$\$\$}P < 0.001$; $^{****, \#\#\#\#, \$\$\$\$}P < 0.0001$. Scale bars in A-D are 1 mm.

EdU cell proliferation assay

EdU cell proliferation assays were performed with the EdU Cell Proliferation Assay kit (Beyotime, Shanghai, China). Cells were seeded at 5×10^3 per well in 6-well plates 24 h before treatment. Then EdU (20 mmol/L) solution was added to each well and incubated for 2 h. Cells were subsequently fixed in 4% paraformaldehyde for 1h at room temperature following treatment with 0.3% Triton X-100 for an hour. Following PBS washing, the cells were incubated with Click solution for 30 min. Next, cell nuclei were counterstained with Hoechst at room temperature for 10 min. The cells were then stained using Hoechst solution. The total number of cells and EdU-positive cells were counted at random in three high-magnification fields under the microscope, and the percentage of EdU-positive cells was determined.

Quantitative real-time PCR

Trizol reagent (catalog no.: 9108; Takara) was used to extract total RNA from VSMCs. 1 μg aliquots were then reverse transcribed into complementary DNA (catalog no.: PR047; Takara). Quantitative real-time PCR using SYBR Green reagent (catalog no.: PR802A; Takara) was carried out according to the manufacturer's instructions. Primers were purchased from Takara.

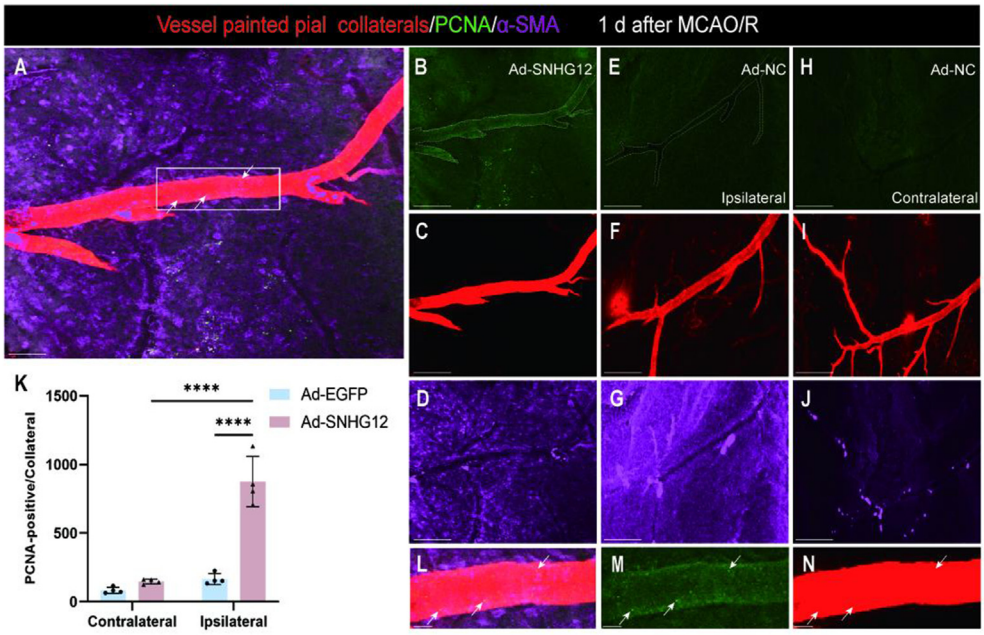

Fig. 3. Increased cell proliferation within the MCA-ACA collateral niche of Ad-SNHG12 mice 1 day after MCAO/R. High magnification confocal imaging was used to view vessel-painted brains that had been immunolabeled with anti-PCNA (green; white arrows) and anti-αSMA (purple). Cell division in the ipsilateral (A–G) and contralateral (H–I) hemispheres was examined for collateral remodeling 1 day after MCAO/R using maximum Z-projection analysis of the whole Z-stacked vessel. (A) Representative 3D projected picture from vessel painted (red) ipsilateral Ad-SNHG12 pial surface of MCA-ACA collateral with PCNA and α-SMA antibodies. Ad-SNHG12 collateral vessels have more aligned $PCNA^+$ cells than Ad-NC. (B–D) Representative single-channel photos of A that show the expression of PCNA and α-SMA in the Ad-SNHG12 collater (E–G). No PCNA staining was seen in the contralateral pial collaterals of the same representative injured Ad-NC animal (H–I). (K) Quantified data shows that Ad-SNHG12 mice have more $PCNA^+$ cells in the collateral vessel wall. (L–N) High-magnification confocal ortho pictures of Ad-SNHG12 collateral wall cell division from inset in A. Scale bars: 50 μm (A–J) and 10 μm (L–N). Two-way ANOVA with Bonferroni's post hoc test; n = 4–5 mice per group; 4–5 MCA-ACA collaterals were analyzed per mouse. $^{****}P < 0.0001$.

The primer sequences are as follows:
β-actin-forward: CCTAGGCACCAGGGTGTGAT
Reverse: CTTCTCCATGTCGTCCAGT
SNHG12-forward: TCTGGTGATCGAGGACTTCC
Reverse: ACCTCCTCAGTATCACACACT

Western blot

Western blot analysis was carried out as previously described [11]. RIPA lysis buffer (catalog no.: PM0013B; Beyotime) was used to extract proteins in a specific proportion from primary VSMCs or brain tissues. Following centrifugation, the supernatant was collected, and the protein content was determined with the BCA kit (catalog no.: P0012; Beyotime). Subsequently loading equal amounts of total protein onto SDS-PAGE gels, they were transferred to 0.45 μm PVDF membranes (Millipore, Billerica, MA) and blocked with 5% nonfat milk for 1h. Primary antibodies against RGMa (1:10,000 dilution; catalog no.: ab169761; abcam), SM22α (1:2000 dilution; catalog no.: ab14106; abcam), α-SMA (1:1000 dilution; catalog no.: 19245; CST), OPN (1:1000 dilution; catalog no.: 25715-1-AP; Proteintech, China) and MMP9 (1:1000 dilution; catalog no.: 10375-2-AP; Proteintech, China) were incubated at 4 °C overnight. Goat anti-mouse (1:5000 dilution; catalog no.: SA00001-1; Proteintech, China) or goat anti-rabbit (1:5000 dilution; catalog no.: SA00001-2; Proteintech, China) secondary antibodies were added and incubated for 1 h at room temperature. The images were captured and quantified by the Gel imaging analyzer system (version GelDoc GO; BIO-RAD, United States).

Statistical analysis

Statistics were performed with GraphPad Prism 9.0 and SPSS 26.0 (IBM). All data are derived from at least three independent experiments. The student's t-test and one-way repeated-measures ANOVA were used to compare groups and subgroups. Nonparametric data were analyzed using the chi-square and Mann-Whitney U tests. A difference was considered statistically significant at $P < 0.05$.

Results

SNHG12 enhances CBF, neuronal organization, and behavioral recovery following middle cerebral artery occlusion reperfusion (MCAO/R)

Our initial analysis showed that SNHG12 expression was elevated after MCAO/R (Fig. 1, A). Then, we used Ad-SNHG12 to induce overexpression of SNHG12 expression (Supplemental Figure S1). We subsequently found that SNHG12 significantly decreased infarct volume versus controls at 4 days after MCAO/R (20.95 ± 5.90 mm^3 vs. 38.85 ± 4.10 mm^3) (Fig. 1B and C). These findings are consistent with the elevated CBF generated by SNHG12. Laser Doppler was further used to determine CBF in the ipsilateral cerebral hemisphere before, and 1–4 days after MCAO/R. The measured perfusion units (PFUs) were then compared with the baseline pre-injury CBF (Fig. 1D and E). Overall, we discovered a significant increase in CBF at 1 day (57.66 ± 7.11 vs. 24.93 ± 10.34), 2 days (73.71 ± 5.29 vs. 47.12 ± 6.49), 3 days (84.92 ± 4.97 vs. 59.39 ± 5.39), and 4 days (101.28 ± 6.35 vs. 76.99 ± 3.46) in the Ad-SNHG12 groups compared with Ad-NC groups. We also observed enhanced behavioral recovery in the Ad-SNHG12 group. Rotarod testing showed significant improvements in motor performance in the Ad-SNHG12 group compared to that in the Ad-NC group 4 days after MCAO/R, with slight gains also observed at 7 days (Fig. 1F). Subsequently, we used neurological severity scoring to investigate the effect of SNHG12 on neural functional defects in MCAO/R. We observed a significant difference in the NSS of mice in Ad-SNHG12 groups compared with the Ad-NC group at 1 days (6.25 ± 0.70 vs. 8.12 ± 0.64), 4 days (4.50 ± 0.53 vs. 6.50 ± 0.53), and 7 days (3.00 ± 0.75 vs. 4.75 ± 0.70) (Fig. 1G). These results indicate that SNHG12 plays a role in functional impairment and brain tissue damage after MCAO/R.

SNHG12 promotes leptomeningeal collaterals remodeling after MCAO/R

To determine whether pial collateral remodeling correlated with CBF and behavioral recovery, we performed vessel painting 1 and 4 days after

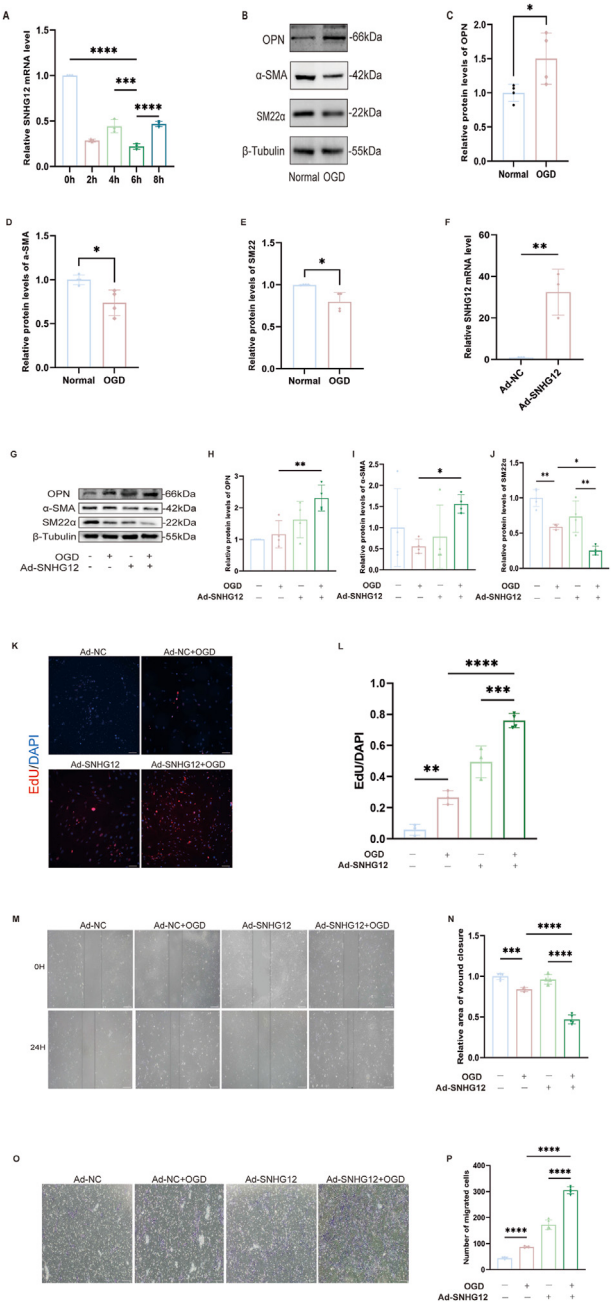

Fig. 4. SNHG12 mediates the dedifferentiation, proliferation, and migration of VSMCs after OGD/R. (A) The relative SNHG12 mRNA levels in the primary mice VSMCs treated with gradient OGD/R (0, 2, 4, 6, and 8 h). n = 3. (B–E) Western blot analysis (B) and quantification of the relative protein expression of OPN (C), α-SMA (D), and SM22α (E) in primary mice VSMCs cultured with OGD/R. n = 4. (F) Relative mRNA levels of SNHG12 after adenovirus overexpression in primary mice VSMCs. n = 3. (L and K) Edu was used to measure VSMC proliferation. The VSMCs were cultured in different conditions (Ad-NC, Ad-NC + OGD, Ad-SNHG12, and Ad-SNHG12 + OGD) n = 5. (M and N) OGD-induced VSMCs, treated with Ad-SNHG12 or Ad-NC, underwent wound healing experiments. n = 4–5. (O and P) The same treated VSMCs (Ad-NC, Ad-NC + OGD, Ad-SNHG12, and Ad-SNHG12 + OGD) were submitted to a transwell chamber test to assess the migration ability of VSMCs. n = 4–5. $^{*}P < 0.05$, $^{**}P < 0.01$, $^{***}P < 0.001$; $^{****}P < 0.0001$; the scale bar represents 100 μm.

stroke in both the Ad-SNHG12 and Ad-NC groups. Overall, we detected an increase in the ipsilateral pial collateral diameter compared with the contralateral diameter in both Ad-SNHG12 (Fig. 2A and B) and Ad-NC (Fig. 2C and D) mice. However, SNHG12 significantly accelerated the remodeling of MCA-ACA inter-collaterals 1 day (Ad-SNHG12 33.72 ± 5.89 μm vs. Ad-NC 19.28 ± 2.19 μm) and 4 days (Ad-SNHG12 49.69 ± 3.91 μm vs. Ad-NC 31.76 ± 2.29 μm) following MCAO/R (Fig. 2E). We further assessed the intercollaterals because the PCAs could potentially provide retrograde reperfusion to the area affected by the blocked MCAs. Measurements of MCA-PCA connected revealed wider collateral diameters in the Ad-SNHG12 versus the Ad-NC group at both 1 day (36.02 ± 5.00 μm vs. 20.75 ± 1.37 μm, separately) and 4 days (49.09 ± 6.48 μm vs. 31.76 ± 2.29 μm, separately) (Fig. 2F). The cumulative diameter of all inter-collaterals (collaterals connecting the MCA-ACA and MCA-PCA major branches) was larger in in the Ad-SNHG12 compared to the Ad-NC group at 1 day (34.87 ± 5.34 μm vs. 20.01 ± 1.63 μm, respectively) and 4 days (49.13 ± 4.83 μm vs. 32.19 ± 1.69 μm, respectively) (Fig. 2G). A significant difference in the total number of intercollaterals was further detected after MCAO/R (Fig. 2H), indicating that SNHG12 not only improved CBF through side branch remodeling but also by including more side branches, as demonstrated by the total number of side branch gaps. Furthermore, analysis of the collateral size revealed that the ipsilateral Ad-SNHG12 group had the largest increase in collateral diameter. At 1 day after MCAO/R, 84% of collaterals were larger than 31 μm, with this number increasing to 91% at 4 days. In contrast, less than 10% of collaterals on the contralateral side were above 31 μm. However, fewer than 10% of the Ad-NC ipsilateral collaterals measured longer than 31 μm at 1 day, while 83% achieved this at 4 days following MCAO/R. Moreover, a higher percentage of Ad-SNHG12 collaterals had a size larger than 50 μm: 33% compared to under 10% in Ad-NC groups (Fig. 2I and J).

Early cellular remodeling evidence in vessel-painted collaterals

To investigate whether SNHG12 improved early remodeling of pial vessels by enhancing SMC growth properties, we performed immunostaining for the smooth muscle cell-specific marker (α-SMA) and cell division marker (PCNA) on Ad-SNHG12 and Ad-NC cortical tissue whole mounts 1 day following MCAO/R and vessel painting (Fig. 3). Examination of the maximum intensity z-stack confocal images revealed that Ad-SNHG12 mice exhibited higher numbers of PCNA cells in the MCA-ACA pial ipsilateral collateral vessel wall than in the Ad-NC ipsilateral and Ad-SNHG12 contralateral vessels. Overall, these data indicate that SNHG12 may facilitate early remodeling by enhancing smooth muscle cell proliferation in the collateral territory.

SNHG12 upregulation improves the dedifferentiation of contractile VSMCs

SNHG12 exhibited the most notable drop at the 6-h time point following oxygen-glucose deprivation/reoxygenation (Fig. 4, A). Therefore, subsequent OGD tests were scheduled for 6 h. Following OGD/R treatment, cells gradually dedifferentiated into a synthetic phenotype, characterized by an increase in the proliferative marker CD68 and a decrease in the expression of the contractile markers SM22α and α-SMA (Fig. 4, B–E). The expression of SNHG12 in mouse primary VSMCs was upregulated by Ad-SNHG12, and the expected increase in SNHG12 expression was confirmed using PCR (Fig. 4, F). Western blot examination revealed further reduced levels of the VSMC contractile markers SM22α and α-SMA, in addition to elevated levels of the proliferative marker OPN in the OGD/R-stimulated VSMCs with upregulated SNHG12 (Fig. 4G–J). Wound healing, Transwell, and Edu assays demonstrated enhanced proliferation and migration in OGD/R-stimulated VSMCs with elevated SNHG12 levels (Fig. 4, K–P). SNHG12 upregulation further enhances OGD/R-induced proliferation, migration, and dedifferentiation of VSMCs.

SNHG12 upregulates MMP9 expression in the dedifferentiation of VSMCs for lateral vascular remodeling

During vascular remodeling, MMP9 might enhance VSMC migration by interacting with integrins [12]. The possibility that SNHG12 regulates

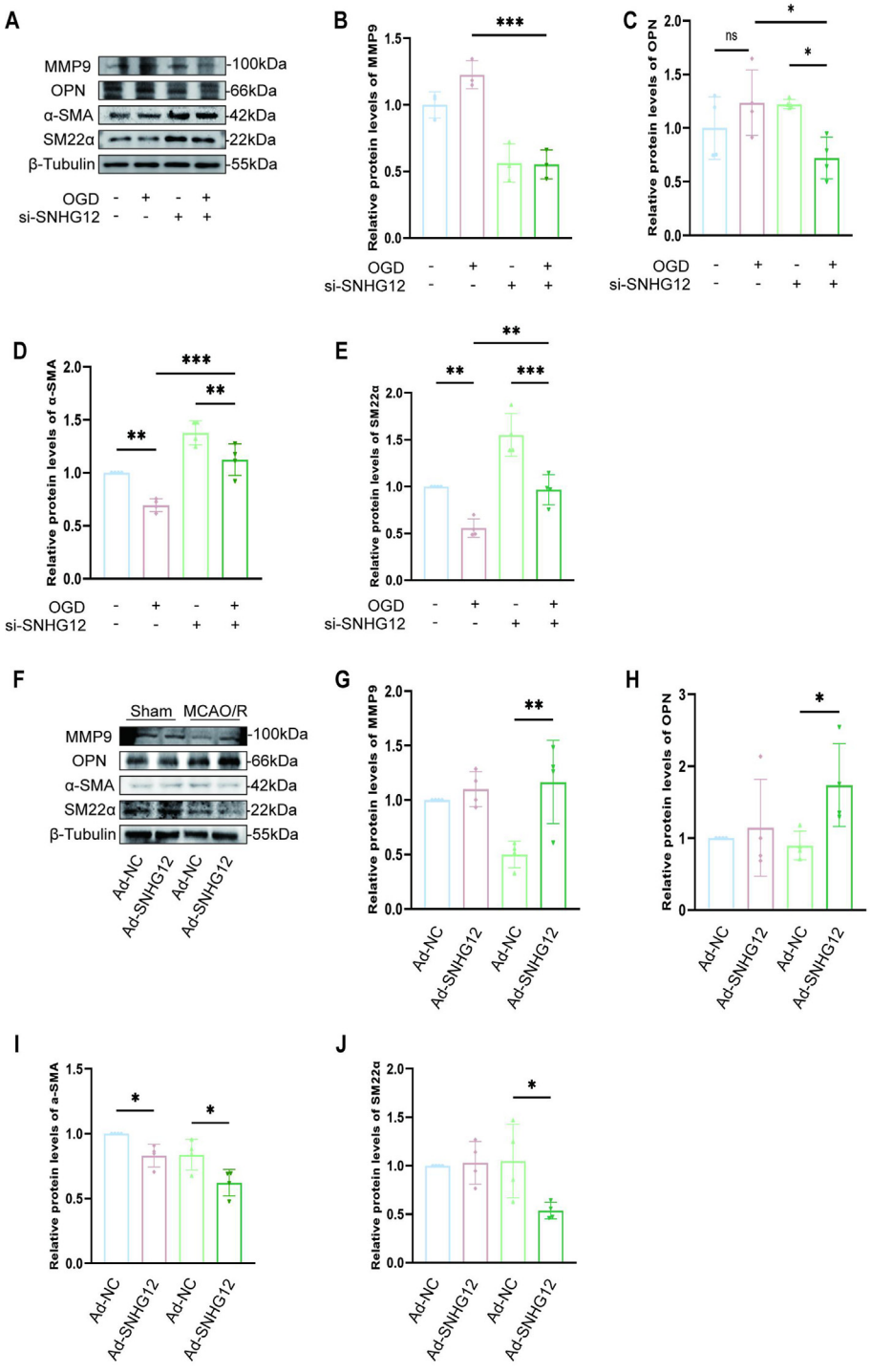

Fig. 5. SNHG12 stimulates MMP9 expression in VSMCs during dedifferentiation for lateral vascular remodeling. (A–E) Western blot analysis (A) and quantification for the relative protein expression of MMP9 (B), OPN (C), α-SMA (D), and SM22α (E) in the primary mice VSMCs transfected with si-SNHG12 or si-NC, followed by or not OGD/R. n = 5. (F–J) Western blot analysis (F) from ipsilateral hemisphere lysates 4 days after MCAO/R. There is significantly elevated MMP9 (G) and OPN (H) protein in Ad-SNHG12 mice lysates compared with Ad-NC mice. While Ad-SNHG12 mice have reduced α-SMA (I), and SM22α (J) expression compared with Ad-NC mice. n = 4. One-way ANOVA with Bonferroni's post hoc test. $^{*}P < 0.05$, $^{**}P < 0.01$, $^{***}P < 0.001$.

MMP9 was therefore investigated. First, the protein expression of MMP9 was found to decrease in OGD/R VSMCs after SNHG12 silencing (Fig. 5A–C). This was accompained by increased protein levels of VSMCs contractile indicators and decreased protein levels of proliferative markers (Fig. 5D–F). Furthermore, Western blot examination revealed that SNHG12 overexpression in MCAO/R-treated animals enhanced the dedifferentiation of contractile VSMCs, as demonstrated by elevated levels of the proliferative marker OPN and reduced levels of the VSMC contractile markers SM22α and α-SMA. However, the effect was counteracted by SNHG12 knockdown, as evidenced by the decrease in MMP9, the decrease in proliferation markers, and the increase in contraction markers (Fig. 5L–Q). Therefore, SNHG12 stimulated MMP9 expression and contractile VSMC dedifferentiation.

SNHG12 enhances MMP9 in the dedifferentiation of VSMCs through RGMa

We observed that OGD/R increased the dedifferentiation of contractile VSMCs into a synthetic phenotype associated with increased levels of MMP9 and RGMa (Fig. 6A–F). While protein expression of MMP9 decreased in OGD/R-induced VSMCs when RGMa was silenced (Fig. 6G–H). Meanwhile, the dedifferentiation of VSMCs treated with OGD/R was impeded by RGMa silencing, as indicated by the observed

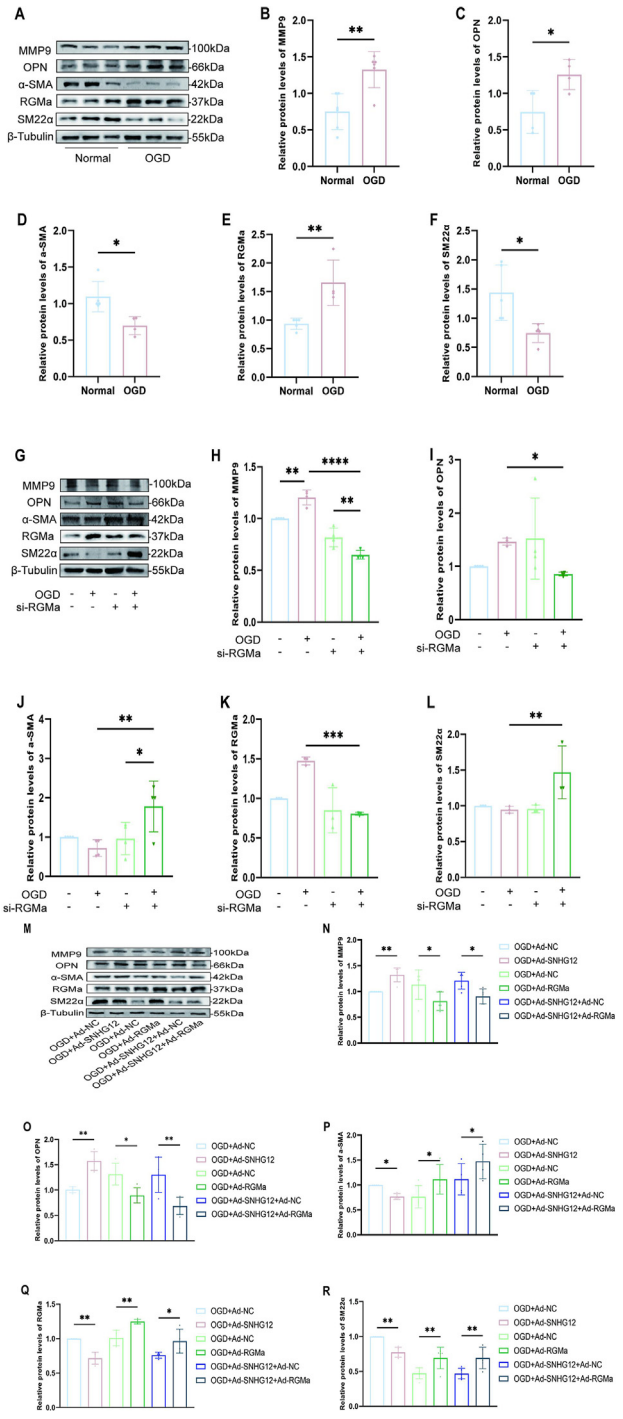

Fig. 6. RGMa overexpression reverses the dedifferentiation of OGD/R-induced VSMCs promoted by SNHG12 overexpression. (A–F) Western blot analysis (A) and quantification for the relative protein expression of MMP9 (B), OPN (C), α-SMA (D), RGMa(E), and SM22α (F) in the primary mice VSMCs treated with or not OGD/R. n = 4. (G–L) Western blot analysis (G) and quantification for the relative protein expression of MMP9 (H), OPN (I), α-SMA (J), RGMa (K), and SM22α (L) in the OGD/R-induced primary mice VSMCs treated with si-RGMa or si-NC. n = 4. (M–R) Western blot analysis (M) and quantification for the relative protein expression of MMP9 (N), OPN (O), α-SMA (P), RGMa(Q), and SM22α (R) in the primary mice VSMCs treated with different conditions (OGD + Ad-NC, OGD + Ad-SNHG12, OGD + Ad-NC, OGD + Ad-RGMa, OGD + Ad-SNHG12 + Ad-NC, and OGD + Ad-SNHG12 + Ad-RGMa). n = 4. *P < 0.05, **P < 0.01.

decrease in OPN and the upregulation of SM22α and α-SMA levels (Fig. 6G–L). Furthermore, to investigate whether RGMa mediates the regulation of MMP9 by SMHG12, and thus participates in the dedifferentiation of contractile VSMCs, we applied Ad-SNHG12 and Ad-RGMa to overexpress SNHG12 and RGMa in OGD/R-treated VSMCs. Western blot ananlysis further demonstrated that SNHG12 overexpression upregulated MMP9 expression, and facilitated the dedifferentiation of VSMCs treated with OGD/R. However, this effect was counteracted by Ad-RGMa treatment (Fig. 6M–R). These results show that RGMa is involved in the process by which SNHG12 influences MMP9 to foster the transformation of contractile VSMCs into a synthetic phenotype.

Discussion

Arterial remodeling, which is induced by modifications in the characteristics of VSMCs, is an essential component of vascular injury. However, the molecular mechanisms underlying this complex pathophysiologic process remain unclear. In this study, we show how SNHG12 regulates the dedifferentiation of constricted VSMCs toward the synthetic phenotype, a process which promotes cerebrovascular collateral remodeling after cerebral ischemia-reperfusion.

Ischemia-reperfusion disrupts intravascular oxygen balance, triggering the release of reactive oxygen species (ROS) and free radicals. This drives the overexpression of proinflammatory factors, causing major damage to vascular endothelial cells and smooth muscle cells [13,14]. VSMCs play a crucial role in vascular remodeling and collateral vessel maturation. Prior research has shown that SNHG12 is a key regulator of tumor, cerebrovascular injury, and angiogenesis [15,16]. Although SNHG12 promotes neovascularization, its role in arterial remodeling remains unclear. In this study, we found that the expression of SNHG12 increased following cerebral ischemia-reperfusion injury but rather decreased in primary smooth muscle cells following OGD/R treatment. Simultaneously, overexpression of SNHG12 reversed the dedifferentiation of contractile VSMCs induced by OGD/R in vitro, thus promoting proliferative migration and dedifferentiation. In vivo, overexpression of SNHG12 increased the density and diameter of molluscum contagiosum arteries. We therefore hypothesized that SNHG12 would be downregulated in primary smooth muscle cells cultured alone following OGD/R treatment in vitro. However, in the mouse model of cerebral ischemia-reperfusion, we observed a complex pathophysiological process, in which multiple cells expressing SNHG12 exerted protective effects. This triggered an overall increase in SNHG12 levels after stroke.

MMP-9 is a zinc-dependent metalloproteinase involved in extracellular matrix degradation and remodeling, which plays important roles in angiogenesis and vascular remodeling [17]. Higher MMP-9 concentrations have further been found to be associated with good collateral status in acute ischemic stroke patients with cerebral large artery atherosclerosis [18]. For example, Zorina et al. [19] showed that the effect of MMP-9 deficiency on geometric remodeling was caused by changes in collagen metabolism and structure. MMPs, especially MMP-9, are also associated with outward arterial remodeling [12,20]. Marimastat, a broad-spectrum inhibitor, has further been shown to reduce constrictive arterial remodeling following balloon angioplasty in a pig model by inhibiting MMP [21]. MMP-9 has also been shown to bind to fibrin in vitro, and may drive VSMC migration following injury by releasing chemotactic peptides and localizing MMP9 activity to unstable atherosclerotic plaques [22]. MMP9 can also alter cell-matrix binding properties and enhance cell migration without activation or proteolysis. By interacting with MMP-9 receptors, such as CD44, MMP-9 can also promote SMC binding to the matrix without destroying type I collagen [23,24].

RGMa is a glycosylphosphatidylinositol-anchored membrane glycoprotein involved in atherosclerosis and injury-induced remodeling [25]. Li *et al.* [26] showed that the role of RGMa in the blood-brain barrier disruption may be associated with MMP9. Yuan *et al.* [25] showed that RGMa facilitated the dedifferentiation of VSMCs into macrophage-like

cells by improving the function of Slug via the MEK-ERK1/2 signaling pathway. Zhang *et al.* [27] also discovered that RGMa reduced the expression of VEGF and *p*-FAK (Tyr397) by reducing neopterin and Unc5b expression in vitro, thereby resulting in the inhibition of endothelial cell proliferation, tube formation, and migration. Wang *et al.* [28] also found that RGMa inhibited angiogenesis via VEGF, Ang2, Ang1, and BDNF following cerebral ischemia/reperfusion injury. In this study we investigated whether SNHG12 stimulates contractile VSMC dedifferentiation by upregulating MMP9 expression. In vitro, MMP9 expression was elevated in primary VSMCs treated with OGD/R and reduced in OGD/R-treated VSMCs following SNHG12 silencing. The reason that MMP9 was not significantly increased in Fig. 5 may be that SNHG12 was knocked down using siRNA prior to OGD treatment. The decrease in SNHG12 expression may have led to a decrease in MMP9 that was greater than the upregulation of MMP9 by OGD treatment alone. We found that RGMa expression was reduced in VSMCs overexpressing SNHG12 after OGD/R treatment. Indeed, RGMa overexpression reversed the phenotypic dedifferentiation mediated by SNHG12 overexpression in OGD/R-treated VSMCs. The current study revealed that OGD/R-induced VSMCs increased MMP9 expression accompanied by increased RGMa. In contrast, RGMa overexpression reduced the expression of MMP9 and VSMCs proliferation markers. Thus, SNHG12 appears to regulate MMP9 during VSMC dedifferentiation from the contractile to the synthetic phenotype via action on RGMa, enhancing collateral artery remodeling following ischemia-reperfusion. Indeed, one previous study observed that reduced RGMa levels decreased the role of MMP9 in the blood-brain barrier (BBB), thereby attenuating BBB dysfunction [26]. Two possible explanations have been proposed to explain the different changes in RGMa levels in the BBB and VSMCs. Second, MMP9 involvement varies among studies. The blood-brain barrier is broken by the MMP9-mediated digestion of the basement membrane of cerebral microvascular endothelial cells and alteration of tight junctions, whereas VSMCs are stimulated to interact with newly formed basement membranes, triggering intracellular signaling via integrins to induce phenotypic switching and sustained migration.

The current study enriches our understanding of how SNHG12 affects cellular function, and further reveals the mechanisms that induce specific adaptive responses in collateral circulation. Why some patients show more collateral circulation openings than others following stroke still remains unknown. Understanding the underlying mechanisms is crucial for developing approaches to predict the collateral involvement and improve the prognosis of ischemic stroke.

Author Contributions

A. J., Q. W., and X. Q. conceptualization; A. J., Z. W., and X. Q. methodology; R. C. and S. Z. formal analysis; A. J. and R. C. investigation; A. J. and X. Q. writing-original draft.

Declaration of competing interest

The authors declare that they have no conflicts of interest with the contents of this article.

Data availability

Data used in this study are available from Anan Jiang by request (E-mail: 1769278944@qq.com).

Acknowledgments

The authors gratefully acknowledge the financial support of the following foundation committees. This study is supported by The First Affiliated Hospital of Chongqing Medical University's Basic Research Project, China (grant no.: cyyy-xkdfjh-jcyj-202309),Chongqing Medical Scientific Research Project (Joint Project of Chongqing Health Commission and Science and Technology Bureau), China (grant no.: 2023MSXM005) and The Natural Science Foundation of Sichuan Province, China (grant no.: 24NSFSC2240).

Appendix A. Supplementary data

Supplementary data to this article can be found online at https://doi.org/10.1016/j.neurot.2024.e00429.

References

[1] Iwasawa E, Ichijo M, Ishibashi S, Yokota T. Acute development of collateral circulation and therapeutic prospects in ischemic stroke. Neural Regen Res Mar 2016;11(3):368–71. https://doi.org/10.4103/1673-5374.179033.
[2] Seyman E, Shaim H, Shenhar-Tsarfaty S, Jonash-Kimchi T, Bornstein NM, Hallevi H. The collateral circulation determines cortical infarct volume in anterior circulation ischemic stroke. BMC Neurol Oct 21 2016;16(1):206. https://doi.org/10.1186/s12883-016-0722-0.
[3] Lima FO, Furie KL, Silva GS, Lev MH, Camargo ECS, Singhal AB, et al. The pattern of leptomeningeal collaterals on CT angiography is a strong predictor of long-term functional outcome in stroke patients with large vessel intracranial occlusion. Stroke Oct 2010;41(10):2316–22. https://doi.org/10.1161/strokeaha.110.592303.
[4] Heil M, Schaper W. Influence of mechanical, cellular, and molecular factors on collateral artery growth (arteriogenesis). Circ Res Sep 3 2004;95(5):449–58. https://doi.org/10.1161/01.Res.0000141145.78900.44.
[5] Zijie W, Anan J, Hongmei X, Xiaofan Y, Shaoru Z, Xinyue Q. Exploring the potential mechanism of Fritiliariae Irrhosae Bulbus on ischemic stroke based on network pharmacology and experimental validation. Front Pharmacol 2022;13:1049586. https://doi.org/10.3389/fphar.2022.1049586.
[6] Okyere B, Mills 3rd WA, Wang X, Chen M, Chen J, Hazy A, et al. EphA4/Tie2 crosstalk regulates leptomeningeal collateral remodeling following ischemic stroke. J Clin Invest Feb 3 2020;130(2):1024–35. https://doi.org/10.1172/jci131493.
[7] Okyere B, Creasey M, Lebovitz Y, Theus MH. Temporal remodeling of pial collaterals and functional deficits in a murine model of ischemic stroke. J Neurosci Methods Jan 1 2018;293:86–96. https://doi.org/10.1016/j.jneumeth.2017.09.010.
[8] Chen J, Li Y, Wang L, Zhang Z, Lu D, Lu M, et al. Therapeutic benefit of intravenous administration of bone marrow stromal cells after cerebral ischemia in rats. Stroke Apr 2001;32(4):1005–11. https://doi.org/10.1161/01.str.32.4.1005.
[9] Wang Y, Qiao L, Qiu J, Mi W, Han Y, Zhong C. Establishing primary cultures of vascular smooth muscle cells from the spiral modiolar artery. Int J Pediatr Otorhinolaryngol Aug 2012;76(8):1082–6. https://doi.org/10.1016/j.ijporl.2012.02.021.
[10] Narayanan SV, Dave KR, Perez-Pinzon MA. Ischemic preconditioning protects astrocytes against oxygen glucose deprivation via the nuclear erythroid 2-related factor 2 pathway. Transl Stroke Res Apr 2018;9(2):99–109. https://doi.org/10.1007/s12975-017-0574-y.
[11] Dissmore T, Seye CI, Medeiros DM, Weisman GA, Bradford B, Mamedova L. The P2Y2 receptor mediates uptake of matrix-retained and aggregated low density lipoprotein in primary vascular smooth muscle cells. Atherosclerosis Sep 2016;252:128–35. https://doi.org/10.1016/j.atherosclerosis.2016.07.927.
[12] Mason DP, Kenagy RD, Hasenstab D, Bowen-Pope DF, Seifert RA, Coats S, et al. Matrix metalloproteinase-9 overexpression enhances vascular smooth muscle cell migration and alters remodeling in the injured rat carotid artery. Circ Res Dec ;85(12):1179–85. https://doi.org/10.1161/01.res.85.12.1179.
[13] Li CX, Wang XQ, Cheng FF, Yan X, Luo J, Wang QG. Hyodeoxycholic acid protects the neurovascular unit against oxygen-glucose deprivation and reoxygenation-induced injury in vitro. Neural Regen Res Nov 2019;14(11):1941–9. https://doi.org/10.4103/1673-5374.259617.
[14] Hosoo H, Marushima A, Nagasaki Y, Hirayama A, Ito H, Puentes S, et al. Neurovascular unit protection from cerebral ischemia-reperfusion injury by radical-containing nanoparticles in mice. Stroke Aug 2017;48(8):2238–47. https://doi.org/10.1161/strokeaha.116.016356.
[15] Lan T, Ma W, Hong Z, Wu L, Chen X, Yuan Y. Long non-coding RNA small nucleolar RNA host gene 12 (SNHG12) promotes tumorigenesis and metastasis by targeting miR-199a/b-5p in hepatocellular carcinoma. J Exp Clin Cancer Res Jan 10 2017;36(1):11. https://doi.org/10.1186/s13046-016-0486-9.
[16] Zhao M, Wang J, Xi X, Tan N, Zhang L. SNHG12 promotes angiogenesis following ischemic stroke via regulating miR-150/VEGF pathway. Neuroscience Oct 15 2018;390:231–40. https://doi.org/10.1016/j.neuroscience.2018.08.029.
[17] Zbinden S, Wang J, Adenika R, Schmidt M, Tilan JU, Najafi AH, et al. Metallothionein enhances angiogenesis and arteriogenesis by modulating smooth muscle cell and macrophage function. Arterioscler Thromb Vasc Biol Mar 2010;30(3):477–82. https://doi.org/10.1161/atvbaha.109.200949.
[18] Yang B, Ding Y, Liu X, Cai Y, Yang X, Lu Q, et al. Matrix metallopeptidase 9 and placental growth factor may correlate with collateral status based on whole-brain perfusion combined with multiphase computed tomography angiography. Neurol Res Oct 2021;43(10):838–45. https://doi.org/10.1080/01616412.2021.1939238.
[19] Galis ZS, Johnson C, Godin D, Magid R, Shipley HM, Senior RM, et al. Targeted disruption of the matrix metalloproteinase-9 gene impairs smooth muscle cell migration and geometrical arterial remodeling. Circ Res Nov 1 2002;91(9):852–9. https://doi.org/10.1161/01.res.0000041036.86977.14.
[20] de Smet BJ, de Kleijn D, Hanemaaijer R, Verheijen JH, Robertus L, van Der Helm YJ, et al. Metalloproteinase inhibition reduces constrictive arterial

remodeling after balloon angioplasty: a study in the atherosclerotic Yucatan micropig. Circulation Jun 27 2000;101(25):2962–7. https://doi.org/10.1161/01.cir.101.25.2962.
[21] Sierevogel MJ, Pasterkamp G, Velema E, de Jaegere PP, de Smet BJ, Verheijen JH, et al. Oral matrix metalloproteinase inhibition and arterial remodeling after balloon dilation: an intravascular ultrasound study in the pig. Circulation Jan 16 2001;103(2):302–7. https://doi.org/10.1161/01.cir.103.2.302.
[22] Makowski GS, Ramsby ML. Binding of latent matrix metalloproteinase 9 to fibrin: activation via a plasmin-dependent pathway. Inflammation Jun 1998;22(3):287–305. https://doi.org/10.1023/a:1022300216202.
[23] Allan JA, Docherty AJ, Barker PJ, Huskisson NS, Reynolds JJ, Murphy G. Binding of gelatinases A and B to type-I collagen and other matrix components. Biochem J Jul 1 1995;309(Pt 1):299–306. https://doi.org/10.1042/bj3090299. Pt 1.
[24] Yu Q, Stamenkovic I. Localization of matrix metalloproteinase 9 to the cell surface provides a mechanism for CD44-mediated tumor invasion. Genes Dev Jan 1 1999;13(1):35–48. https://doi.org/10.1101/gad.13.1.35.
[25] Yuan X, Xiao H, Hu Q, Shen G, Qin X. RGMa promotes dedifferentiation of vascular smooth muscle cells into a macrophage-like phenotype in vivo and in vitro. J Lipid Res Oct 2022;63(10):100276. https://doi.org/10.1016/j.jlr.2022.100276.
[26] Li M, Wen Y, Zhang R, Xie F, Zhang G, Qin X. Adenoviral vector-induced silencing of RGMa attenuates blood-brain barrier dysfunction in a rat model of MCAO/reperfusion. Brain Res Bull Sep 2018;142:54–62. https://doi.org/10.1016/j.brainresbull.2018.06.010.
[27] Zhang G, Wang R, Cheng K, Li Q, Wang Y, Zhang R, et al. Repulsive guidance molecule a inhibits angiogenesis by downregulating VEGF and phosphorylated focal adhesion kinase in vitro. Front Neurol 2017;8:504. https://doi.org/10.3389/fneur.2017.00504.
[28] Wang Y, Zhang R, Xing X, Guo J, Xie F, Zhang G, et al. Repulsive guidance molecule a suppresses angiogenesis after ischemia/reperfusion injury of middle cerebral artery occlusion in rats. Neurosci Lett Jan 1 2018;662:318–23. https://doi.org/10.1016/j.neulet.2017.10.036.